J. Membrane Biol. 46, 1–25 (1979)

K^+ Conduction Phenomena Applicable to the Low Frequency Impedance of Squid Axon

Ronald D. Grisell and Harvey M. Fishman

Department of Physiology and Biophysics, University of Texas Medical Branch, Galveston, Texas 77550

Received 17 April 1978; revised 17 October 1978

Summary. The observation of peaking in power spectra of K current noise in squid axon (Fishman, H.M., Moore, L.E., Poussart, D.J.M. 1975, *J. Membrane Biol.* **24**:305) led to the calculation of a low frequency K conduction feature in the impedance (admittance) which was confirmed (Fishman, H.M., Poussart, D.J.M., Moore, L.E. & Siebenga, E., 1977, *J. Membrane Biol.* **32**:255). This paper analyzes two physical phenomena, one within and the other outside of the excitable membrane, that might account for the low frequency impedance (admittance) feature. The accumulation of potassium ions in a space outside the axon in conjunction with diffusion through the Schwann cell layer produces a low-frequency mode that is similar in some respects to that observed experimentally. Alternatively, a hypothetical inactivation process, with a voltage-dependent time constant, associated with conduction in potassium channels gives a better account of the data. Either or both of these phenomena could be involved in producing the low-frequency impedance behavior in the squid axon.

A new low-frequency (1–30 Hz) feature in the complex impedance of squid axon was measured recently (*see* Fig. 1). This feature is of significance to a description of potassium ion conduction in an axon because it was shown to be dependent only upon the state of K conduction, and it cannot be obtained from the linearized Hodgkin-Huxley equations by adjustment of parameters (Fishman *et al.*, 1977*b*; Poussart, Moore & Fishman, 1977). The low-frequency mode is indicative of a rate process that is more complicated than the single first-order process contained in the HH formulation. Furthermore, this impedance feature provides a plausible link to the observation of sharp corners (peaking) in power density spectra of K^+ current noise (Fishman *et al.*, 1975, 1977*a*, *b*) from which it was suggested that K conduction kinetics are not first order. However, with respect to models of K conduction, Fishman *et al.* (1977*b*) state that it is important to distinguish (i) the overall K conduction process in an axon, which includes phenomena arising from structures

0022-2631/79/0046-0001 $05.00

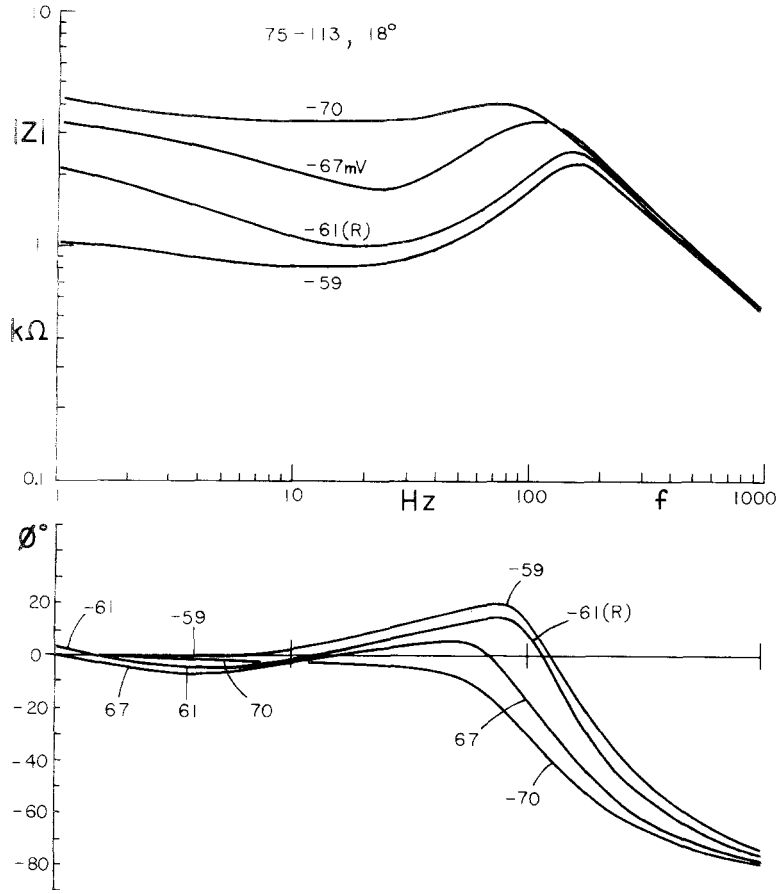

Fig. 1. Representative complex impedance (magnitude and phase) data of squid axon at potentials about rest (R). The low frequency (1–30 Hz) behavior ("dip" in $|Z|$ and negative ϕ) is not contained in the linearized Hodgkin-Huxley equations and is the focus of this paper. An important feature with respect to suitability of applicable models is that the intermediate frequency of zero-phase crossing moves to the left with depolarization from −67 mV. (From Fishman *et al.*, 1977*b*). Membrane area approximately 0.2 cm^2

surrounding the axon, from (ii) phenomena that occur exclusively in the excitable membrane. It is to this problem that this communication is directed.

The complex admittance of two classes of phenomena are calculated and compared with the previously reported impedance (admittance) data. The first phenomenon involves an extra-membrane process generally known as diffusion polarization (Neumcke, 1971) in which the K concentration outside of the excitable membrane changes during current flow as a consequence of an external diffusion barrier. DeGoede *et al.* (1977) have calculated recently that K accumulation could account for

peaking in power spectra of K conduction fluctuations. The second process considered is the effect of a hypothetical inactivation of membrane K channels. K accumulation in conjunction with diffusion through the Schwann cell layer (SCL) produces a low-frequency feature that is similar in some respects to the measured impedance. Alternatively, a hypothetical inactivation process can account for all aspects of the measured impedance function. Nevertheless, both of these phenomena could be involved to some extent.

Symbols and Abbreviations

AF = Adelman & FitzHugh, 1975.
APS = Adelman, Palti & Senft, 1973.
PPS = phenomenological periaxonal space of APS.
HH = Hodgkin & Huxley, 1952.
FH = Frankenhaeuser & Hodgkin, 1956.
GS = Geren-Schmitt space.
AX = axolemma.
H1 = first hypothesis of FH.
H2 = second hypothesis of FH.
SCL = Schwann cell layer.
θ = PPS thickness, in Å.
K_i, K_{se} = potassium (K^+) concentrations, in axoplasm and near inner surface of the SCL, in mM.
K_{ss}, K_{sa} = steady state (under given conditions) and instantaneous K^+ concentrations in PPS, in mM.
K_s = $K_{sa} - K_{ss}$, or excess K^+ concentration in PPS, in mM.
P_K^s = permeability to K^+ through diffusion barrier between PPS and external bulk solution in $cm \cdot sec^{-1}$.
M = efflux of K^+ through excitable membrane, in $mmol \cdot cm^{-2} \cdot sec^{-1}$.
t = time, in msec.
t_o = time at end of falling phase of a single action potential (AP) beginning at $t=0$.
x = spatial variable used in one-dimensional diffusion, in cm.
p = the Laplace transform variable, complex.
l = diffusion path length in several of the diffusion models, in cm.
$K(x,t)$ = a general potassium concentration exterior to AX.
τ = characteristic time in the first hypothesized model of FH, H1, in sec.
D = diffusion coefficient of SCL, in $cm^2\ sec^{-1}$.
M_K, M = K^+ flux into the PPS through the excitable membrane, and outward through the external barrier (including SCL) in $mmol \cdot cm^{-2} \cdot sec^{-1}$.
F = Faraday, 96,486.7 C/mole.
I_M = excitable membrane current including all ions, in $\mu A \cdot cm^{-2}$, positive outward.
I_{Na}, I_K, I_L = ionic current densities, L denoting the Hodgkin-Huxley (HH) leakage, in $\mu A \cdot cm^{-2}$.
t_K = transport number for K^+ through SCL and/or external barrier.
g_{Na}, g_K, g_L = conductances of respective ionic current components, in $mS \cdot cm^{-2}$.

m, h, n = HH parameters, dimensionless, between 0 and 1.
i = hypothesized potassium inactivation parameter, dimensionless.
V_{Na}, V_K, V_L = reversal potentials for respective ionic currents, mV.
g_M = total membrane conductance, $mS \cdot cm^{-2}$.
V_M = potential difference across excitable membrane, inside minus outside, in mV.
V_{tot} = potential of axoplasm relative to 0 reference as external bathing solution or extracellular fluid, in mV.
κ = phenomenological proportionality constant between $F\Delta K_{se}$ and I_M.
R_s = specific resistance in series with HH pathways, in $ohm \cdot cm^2$.

Note: For dimensional consistency in numerical evaluations of Eqs. (1) and (10) in this paper, and Eq. (12) of Adelman and FitzHugh (1975), some of the above dimensioned physical quantities must have factors applied as follows:

Computational $\theta = 10^{-2} \times \theta$	(units of 100 Å)
Computational $P_K^s = 1000 P_K^s$	(units of 10^{-3} cm $\cdot$ sec^{-1})
Computational $M = 10^6 \times M$	(units of 10^{-6} mmole $\cdot$ $cm^{-2} \cdot sec^{-1}$)
Computational $F = 10^{-3} \times F$	(units of 10^3 C $\cdot$ $mole^{-1}$)

All other quantities are entered into equations in the units specified in the list of symbols.

Possible Models for the Low Frequency Feature

Potassium Accumulation

Definite improvements in the descriptions of action potentials in squid axon have been attained (e.g., Frankenhaeuser & Hodgkin, 1956, hereafter FH; Adelman, Palti & Senft, (APS), 1973; Adelman & FitzHugh, (AF), 1975) by incorporating effects of potassium accumulation in the periaxonal space into the Hodgkin-Huxley model (HH). Therefore, it would seem reasonable that some contribution might be noticeable with small signals. It appears that this effect can explain a part of the observed low frequency small signal behavior. Several variations have been proposed and are discussed subsequently.

H1: According to the first hypothesis put forward by FH, there exists a finite aqueous cylindrical space ("periaxonal space"), with thickness θ surrounding the axon membrane, bounded by a concentric and very thin outer barrier to diffusion. Potassium ion concentration in excess of the steady-state concentration, K_s, is assumed to be uniform throughout the space. Outward flow through the barrier is taken to be small in comparison with outward potassium current through the excitable membrane

into the phenomenological space during the falling phase of an action potential (denoted AP). With P_K as the permeability of the outer barrier to potassium ions and M as the potassium through the excitable membrane,

$$\dot{K}_s = \frac{dK_s}{dt} = (M - P_K^s K_s)/\theta. \tag{1}$$

H2: In the second hypothesis of FH, there exists a finite diffusion barrier between the excitable membrane and the external bulk solution, but no aqueous space. The exterior of the membrane is assumed to be in direct contact ($\theta = 0$) with a uniform layer of thickness l, with diffusion coefficient D_2. For solutions to this problem, *see* FH and Crank (1975).

Difficulties with strict adherence to either hypothesis are discussed by FH, who favor H1. It is mentioned (FH) that all evidence at that time probably could have been explained by a combination of H1 and H2, with $50 \leqq \theta \leqq 100$ Å. H1 is then more in agreement with electron micrographic examinations of the periaxonal space (Villegas & Villegas, 1960; Geren & Schmitt, 1954). The major difficulty with H2 is that it predicts a substantial K accumulation during an action potential such that E_K would be reduced significantly. This is contrary to the observed after-potential behavior.

APS: A more recent potassium accumulation model has been developed by Adelman, Palti, Senft and FitzHugh (Adelman & Palti, 1969*a*, *b*; Adelman *et al.*, 1973; Adelman & FitzHugh, 1975), including a phenomenological periaxonal space (PPS), possibly corresponding to "Geren-Schmitt space," the SCL and the external solution. Their system equation is the same as Eq. (1), with the identification of

$$M = M_K - M_e \tag{2}$$

as net flux into the PPS, where

$$M_K = I_K/F \tag{3}$$

and

$$M_e = t_K I_M/F. \tag{4}$$

Here, t_K is the transport number for K^+, I_M is the total membrane current, F is the Faraday, and

$$I_K = g_K(V_M - V_K) \tag{5}$$

is the potassium-ion current, with

$$g_K = \bar{g}_K n^4 \tag{6}$$

and

$$\dot{n} = [\alpha_n(V)(1-n) - \beta_n(V)n]\, T_f \tag{7}$$

and

$$T_f = Q_{10}{}^{(T-6.3)/10}.$$

In the APS model, α_n and β_n are altered somewhat from the functional form of HH, providing a higher value of g_K mainly to account for experimental results (e.g., Fig. 8, Adelman *et al.*, 1973).

Modified APS: In contrast with APS, the present computations will utilize all original HH functions for α_m, β_m, α_h, β_h, α_n and β_n. However, other HH parameters have been changed as noted in figure captions in accordance with the description of K conduction obtained by fits of low frequency impedance data by Fishman *et al.* (1977*b*). A second modification will involve the inclusion of K^+ transport via I_M through the SCL; with distinct transport numbers

$$t_K \equiv \begin{cases} t_{K^{out}} \equiv \dfrac{K_{se}}{K_{se} + Na_{se} + Cl_{se}} & \text{if } I_M > 0 \\ t_{K^{in}} \equiv \dfrac{K_0}{K_0 + Na_0 + Cl_0} & \text{if } I_M < 0 \end{cases} \tag{8}$$

depending on whether I_M is inward or outward. Here, K_{se} is the instantaneous, average K^+ concentration in the PPS. Figure 2 diagrams the situation.

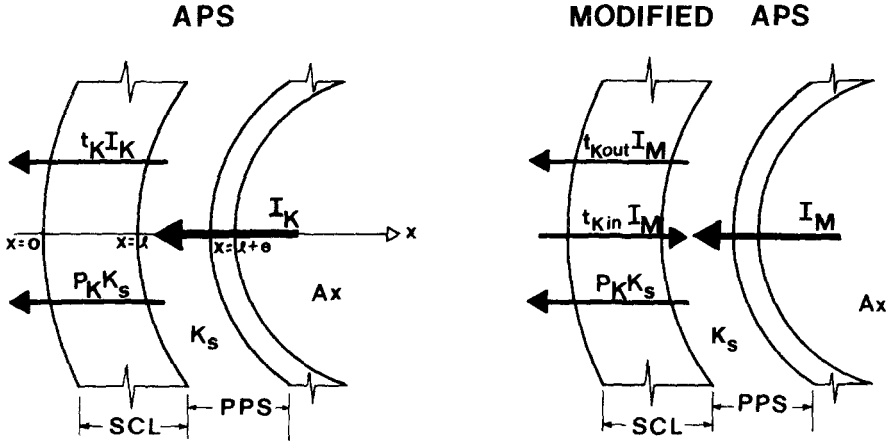

Fig. 2. Schematic comparison of the potassium accumulation models. The spatial variable x is positive to the right and outward current is to the left. *See text* for details

It may well turn out to be necessary for improved fits to modify α_n and β_n if n indeed depends on external potassium concentration (Adelman & Palti, 1969*b*).

The K^+ component of I_M was included as a modification of APS, although it amounts to only a 1–2% correction at rest, primarily to have more accuracy at low frequency and at hyperpolarizations for purposes of modelling. The inclusion of this small component, $t_{K\text{out}} I_M$, (*see* Fig. 2), is also consistent with a return to the original HH functions α_n and β_n, since APS has the effect of increasing g_K due to a change in driving force as a consequence of accumulated K^+ in the PPS. Part of the increase of g_K, as consistent with experimental data, could be due to $t_K I_M$. External concentrations are nominally $K_o = 10$ mM, $Na_o = 460$ mM, $Cl_o = 540$ mM, and K_{se} ranges from about 10.1 to 10.2 mM for a few millivolts depolarization. At rest $t_K = 0.03$, and thus varies about 1% during the recovery phase of an AP. This is in agreement with FH estimates that one AP raises K_{se} about 1.1 mM at 17.5 °C.

Let K_{ss} be the steady state K^+ concentration under maintained conditions and K_{sa} be the instantaneous concentration in the PPS. The *potassium excess concentration* is defined as

$$K_s \equiv K_{sa} - K_{ss}. \tag{9}$$

The APS equation for K_s, modified to include $t_K I_M$ is then:

$$\dot{K}_s = (I_K - t_K I_M - F P_K^s K_s)/(F\theta). \tag{10}$$

In addition to Eq. (7), the other HH system equations are

$$\dot{m} = [\alpha_m(1-m) - \beta_m m]\, T_f \tag{11}$$

$$\dot{h} = [\alpha_h(1-h) - \beta_h h]\, T_f \tag{12}$$

$$I_M = C_M \dot{V} + g_{Na}(V_M - V_{Na}) + g_K(V_M - V_K) + g_L(V_M - V_L) \tag{13}$$

$$g_{Na} = \bar{g}_{Na} m^3 h \tag{14}$$

$$g_K = \bar{g}_K n^4 \tag{15}$$

Equations (7) and (10)–(13) are the system equations for the modified potassium accumulation.

Linearization of a Generalized Model

With little increase of mathematical complexity, the potassium accumulation system can be considered as coupled to the SCL diffusive

system (Adam, 1973), the combined system linearized, and the AC small signal characteristics of either subsystem obtained as special, limiting cases. The general system will also provide for more convenient comparison between FH, APS, AF and inactivation models.

The linearization of Eq. (13) is:

$$\begin{aligned} \Delta I_M = C_M \Delta \dot{V}_M + g_\infty \Delta V_M + \bar{g}_K [4 n_\infty^3 (V_M - V_K) \Delta n - n_\infty^4 \Delta V_K] \\ + \bar{g}_{Na} (3 m_\infty^2 h_\infty \Delta m + m_\infty^3 \Delta h)(V_M - V_{Na}) \end{aligned} \tag{16}$$

$$g_\infty = \bar{g}_{Na} m_\infty^3 h_\infty + \bar{g}_K n_\infty^4 + g_L.$$

The Nernst equation for K^+ reversal potential is

$$V_K = \frac{RT}{F} \ln \left(\frac{K_{ss} + K_s}{K_i} \right),$$

which linearizes as

$$\Delta V_K = \frac{RT}{F} \frac{K_s}{K_{ss}}. \tag{18}$$

Equations (7), (11) and (12) are already linear, but for consistency of notation these can also represent small fluctuations about steady-state values by subtracting right-hand sides evaluated under steady state:

$$\Delta \dot{m} = [A_m \Delta V_M - \Delta m / \tau_m] \tag{19}$$

$$\Delta \dot{h} = [A_h \Delta V_M - \Delta h / \tau_h] \tag{20}$$

$$\Delta \dot{n} = [A_n \Delta V_M - \Delta n / \tau_n] \tag{21}$$

where, with prime denoting differentiation with respect to V_M,

$$A_m = [\alpha_m'(1 - m_\infty) - \beta_m' m_\infty] T_f; \quad \tau_m = (\alpha_m + \beta_m)^{-1} T_f^{-1};$$

$$A_h = [\alpha_h'(1 - h_\infty) - \beta_h' h_\infty] T_f; \quad \tau_h = (\alpha_h + \beta_h)^{-1} T_f^{-1};$$

$$A_n = [\alpha_n'(1 - n_\infty) - \beta_n' n_\infty] T_f; \quad \tau_n = (\alpha_n = \beta_n)^{-1} T_f^{-1}.$$

The effects considered in this paper occur over a limited potential range (± 10 mV about rest potential). Thus phenomena produced by electro-kinetic volume flow through the SCL are negligible according to Adam (1973). The system equation for diffusion through the SCL, considered homogeneous, is

$$\partial K / \partial t = D \partial^2 K / \partial x^2. \tag{22}$$

$K(x, t)$ is the potassium concentration in the SCL at a depth x referenced to $x=0$ at the bulk solution interface (*see* Fig. 2). Equation (22) is coupled to the APS model at the inner surface of the SCL at $x=l$ via equating flux across this boundary:

$$D[\partial K/\partial x]_{x=l}=(I_K-t_K I_M)/F-\theta \dot{K}_s. \tag{23}$$

A boundary condition at the outer surface of the SCL is

$$K(0, t)=K_{se}. \tag{24}$$

K_{se} is the instantaneous deviation from steady state of the potassium concentration near the inner surface of, and within the SCL. As might be expected, the change in K_{se} during accumulation, ΔK_{se}, turns out to be small, being on the order of 0.5 mM. Its effect was investigated using the phenomenological approximation

$$\Delta K_{se} \doteq \kappa[I_M/F] \tag{25}$$

where κ is a proportionality constant. Equation (25) represents a buildup of potassium due to a reflective barrier and follows from the Nernst relation.

The Laplace transform of a function $\Delta f(t)$ will be defined and denoted by

$$\delta f(p)=\int_0^\infty \Delta f(t)\, e^{-pt}\, dt.$$

Operating on both sides of Eqs. (16) and (19)–(22) with the Laplace transform, we obtain

$$\delta I_M=(C_M p+g_\infty)\,\delta V_M+\bar{g}_K\, 4n_\infty^3(V_M-V_K)\,\delta n-\bar{g}_K\, n_\infty^4\, RT(F K_{ss})^{-1}\,\delta K_s$$
$$+\bar{g}_{Na}(3m_\infty^2\, h_\infty\,\delta m+m_\infty^3\,\delta h)(V_M-V_{Na}) \tag{26}$$

$$p\,\delta m=[A_m\,\delta V_M-\delta m/\tau_m] \tag{27}$$

$$p\,\delta h=[A_h\,\delta V_M-\delta h/\tau_h] \tag{28}$$

$$p\,\delta n=[A_n\,\delta V_M-\delta n/\tau_n] \tag{29}$$

$$p\,\delta K=D(d^2\,\delta K/dx^2) \tag{30}$$

the latter having boundary conditions

$$\delta K(0, p)=\delta K_{se} \tag{31}$$

and

$$[\partial \delta K/\partial x]_{x=l}=(\delta I_K-t_K\,\delta I_M)/(FD)-\theta p\,\delta K_s/D. \tag{32}$$

The right-hand side of Eq. (32) will be denoted C in the following. A general solution of Eq. (30) is,

$$\delta \mathrm{K} = \frac{A e^{\gamma_1 x} + B e^{\gamma_2 x}}{\gamma_2 e^{\gamma_2 l} - \gamma_1 e^{\gamma_1 l}} \tag{33}$$

where $\gamma_1 = -\gamma_2 = \sqrt{p/D} \equiv \gamma$

and $A \equiv -\delta \mathrm{K}_{se} \gamma e^{-\gamma l} - C$

$B \equiv C - \delta \mathrm{K}_{se} \gamma e^{\gamma l}$

$C \equiv [d\delta \mathrm{K}/dx]_{x=l}.$

Consequently, Eq. (33) becomes

$$\delta \mathrm{K} = \frac{C \sinh \gamma x + \delta \mathrm{K}_{se} \gamma \cosh \gamma (l-x)}{\gamma \cosh \gamma l}. \tag{34}$$

It will be assumed that K_s does not deviate significantly from the linear, steady-state relationship (18); thus,

$$\delta V_{\mathrm{K}} = \frac{RT}{F \mathrm{K}_{ss}} \delta \mathrm{K}_s. \tag{35}$$

With the definitions of g_n, g_m, and g_h in Fishman *et al.* (1977*b*), Eqs. (26)–(30) and (35) can now be combined and solved to obtain the membrane admittance (*see* Appendix *I* for the derivation of $\hat{Y}_{\mathrm{K}}$).

$$Y_M \equiv \delta I_M / \delta V_M = Y_c + g_L + \hat{Y}_K + Y_{\mathrm{Na}} \tag{36}$$

$$Y_c = p C_M \tag{37a}$$

$$Y_{\mathrm{Na}} = \bar{g}_{\mathrm{Na}} m_\infty^3 h_\infty + \frac{g_m}{1 + p\tau_m} + \frac{g_h}{1 + p\tau_h} \tag{37b}$$

$$\hat{Y}_{\mathrm{K}} = \bar{g}_{\mathrm{K}} n_\infty^4 + \frac{\hat{g}_n}{1 + p\tau_n} + \frac{\hat{g}_{\mathrm{K}}}{1 + p\tau_{\mathrm{K}}} \tag{37c}$$

where

$$\hat{g}_n = g_n \left[1 + \frac{P_{\mathrm{K}}^M (P_{\mathrm{K}} + P_{\mathrm{K}}^M)^{-1} \tau_n}{(\tau_{\mathrm{K}} - \tau_n)} \right] \tag{38a}$$

$$\hat{g}_{\mathrm{K}} = -P_{\mathrm{K}}^M (P_{\mathrm{K}} + P_{\mathrm{K}}^M)^{-1} \left[\bar{g}_{\mathrm{K}} n_\infty^4 + \frac{g_n \tau_{\mathrm{K}}}{(\tau_{\mathrm{K}} - \tau_n)} \right] \tag{38b}$$

and where

$$P_{\mathrm{K}} \equiv \frac{D\gamma}{\tanh(\gamma l)}$$

$$P_{\mathrm{K}}^{M} \equiv \frac{RT}{F^2 \mathrm{K}_{ss}} \bar{g}_{\mathrm{K}} n_{\infty}^4 \left[1 + \frac{D\kappa\gamma}{\sinh(\gamma l)} - t_{\mathrm{K}}\right]$$

$$\tau_{\mathrm{K}} = \theta/(P_{\mathrm{K}} + P_{\mathrm{K}}^{M})$$

$$\kappa \equiv F[\delta \mathrm{K}_{se}/\delta I_{M}].$$

Finally, with the addition of a series resistance element, R_s, to account for experimental conditions, the total admittance becomes

$$Y_{\mathrm{tot}} \equiv Y_M/(1 + R_s Y_M). \tag{39}$$

In the APS limit as $D/l \to P_{\mathrm{K}}^{s}$ (as D and l become proportionally small)

$$D[\partial\, \delta \mathrm{K}/\partial x]_{x=l} = \lim_{l\to 0} D \frac{\delta \mathrm{K}(l,p) - \delta \mathrm{K}(0,p)}{l} = \lim_{l\to 0} (D/l)\, \delta K(l,p) = P_{\mathrm{K}}^{s}\, \delta \mathrm{K}_s \tag{40}$$

since $\delta \mathrm{K}(0,p) \equiv 0$, and Eq. (32) goes over to the Laplace transform of (10), with $\mathrm{K}(l)$ as K_s. Further, in the specialization to the APS model, $\kappa = 0$.

Thus,

$$\frac{1}{\gamma}\tanh(\gamma l) \to l$$

$$\frac{D\kappa\gamma}{\sinh(\gamma l)} = 0.$$

Consequently,

$$P_{\mathrm{K}} \to P_{\mathrm{K}}^{s}$$

$$P_{\mathrm{K}}^{M} \to \frac{RT}{F^2 \mathrm{K}_{ss}} \bar{g}_{\mathrm{K}} n_{\infty}^4 (1 - t_{\mathrm{K}}).$$

From Eq. (37*c*), it can be seen that the original g_n branch must be modified and an additional branch added to the original Hodgkin-Huxley equivalent circuit (*see* Fig. 3). The second term, with pole at $-1/\tau_n$, contributes an RL branch, which may be lumped together with the Hodgkin-Huxley potassium RL branch. This effectively increases g_n to $\hat{g}_n$. The third term, with pole at $-1/\tau_{\mathrm{K}}$, contributes an RL branch with negative element values if $\tau_{\mathrm{K}} > \tau_n$. It can be shown that in an equivalent representation, the conductance g_{K} $(= \bar{g}_{\mathrm{K}} n_{\infty}^4)$ is in series with a parallel combination of capacitor and shunt resistor having values

$$R' = -\hat{g}_{\mathrm{K}}\, g_{\mathrm{K}}^{-1} (g_{\mathrm{K}} + \hat{g}_{\mathrm{K}})^{-1} > 0 \tag{41}$$

$$C = -g_{\mathrm{K}}^{2}\, \tau_{\mathrm{K}}\, \hat{g}_{\mathrm{K}}^{-1} > 0. \tag{42}$$

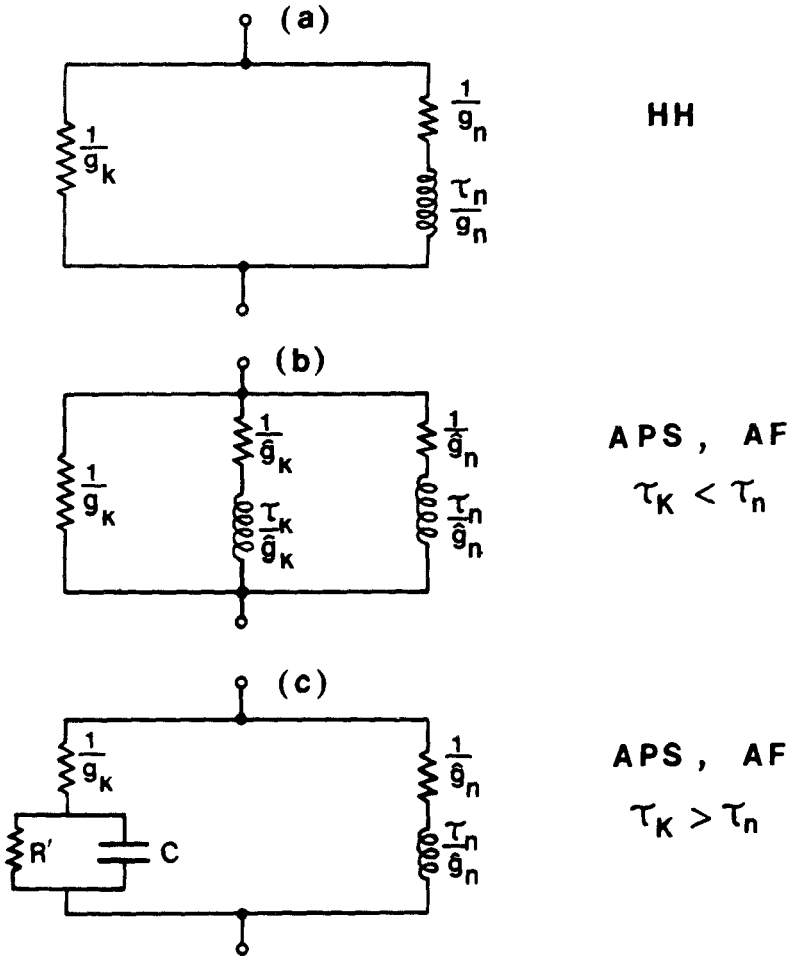

Fig. 3. Electrical circuit description of axon small signal behavior of K conduction. (*a*): From the linearized Hodgkin-Huxley equations. (*b*): Inclusion of K accumulation in an extracellular space according to Adelman *et al.* (1973) and Adelman and FitzHugh (1975). (*c*): Transformation of circuit in *b* to one having positive element values for $\tau_K > \tau_n$. *See text* for definition of parameters

It is of interest to note that an alternative circuit representation for K accumulation has been obtained by de Goede *et al.* (1977) that can also produce peaking in the power spectrum of fluctuations from the K system.

Potassium Inactivation

A possibility quite distinct from the extracellular hypotheses considered so far is that either the long term potassium inactivation observed in

giant axon (Ehrenstein & Gilbert, 1966) produces pertinent effects at characteristic times much shorter than observed (of the order of minutes) or there exists a second inactivation mechanism with more rapid kinetics. A justification for considering a hypothetical K conductance inactivation with $\tau \simeq 30$ msec is based upon the following facts:

In essentially all experimental studies of K conduction, a "droop" occurs in $I_K(t)$ for long duration step clamps. This droop has been considered a nuisance to the experimenter rather than something of phenomenological importance (Adam, 1973). In addition, at long times, polarization of electrodes and aberrations in guarded current measurements (Poussart *et al.*, 1977) complicate the interpretation of data. Furthermore, most experiments have been done at relatively low tem-

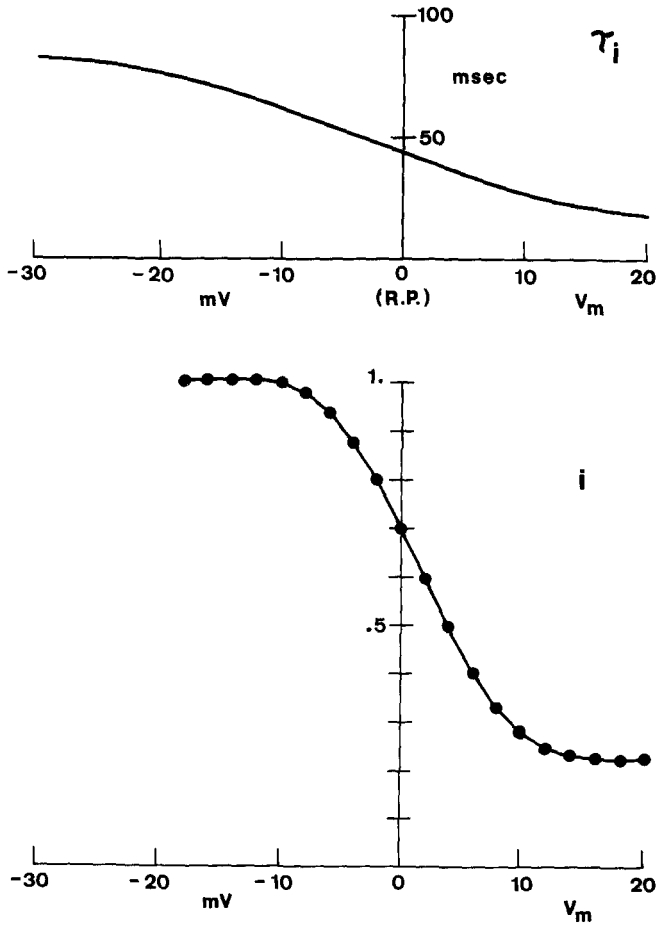

Fig. 4. Potassium inactivation model: $\tau_i(V)$ is the inactivation time constant and i is the inactivation parameter. Both of these are functions of potential as shown

peratures (3–6 °C), whereas the effects that are considered in this paper have been observed only at high temperature (16–18 °C) (Fishman *et al.*, 1977*b*).

Thus, it is not possible, at present, to exclude a K conductance inactivation from consideration as an explanation for the droop in $I_K(t)$ at long times or for the low frequency impedance behavior.

A potassium inactivation could, at least qualitatively, explain the observed low frequency admittance over a limited V_M interval. To demonstrate this, an HH-like expression for inactivation of a branch conductance will be considered

$$g_i = r\,\bar{g}_K\, i_\infty^{r-1}\, n_\infty^4\, \tau_i (V_M - V_K)(\alpha_i' + \beta_i'). \tag{43}$$

Here an arbitrary exponent has been included, although it might be expected that r will not be very different from 1, as in the sodium inactivation. From Eq. (43), g_i is seen to be negative for $V_M > V_K$ if, and only if, the last factor is negative. The parameter i is taken to satisfy a differential equation like (12), hence under steady-state conditions:

$$\alpha_i' - i_\infty(\alpha_i' + \beta_i') = i_\infty'/\tau_i. \tag{44}$$

By Eqs. (43) and (44) g_i is significant only over the bounded interval where n_∞^4 is non-negligible and, at the same time, i_∞' is large negative (*see* Fig. 4, *top*). Figure 4 (*bottom*) shows the inactivation voltage-dependence finally chosen to fit the low-frequency impedance feature. This is not very much different from that of Ehrenstein and Gilbert (1966).

Circuit Considerations

A resistance, R_s, was considered in series with each of the above models, and with various combinations. R_s was usually varied around 7 ohm · cm^2. One additional equation

$$V_M = V_{tot} - I_M R_s \tag{45}$$

is then required to relate V_M to the total potential difference, V_{tot}, between external bathing solution and axoplasm.

A characteristic common to all the models is that the linearizations can be represented in terms of parallel branches effectively across the membrane element. Before discussing the detailed distinctions, therefore, some perspective can be gained by considering the possibilities abstractly

from the point of view of equivalent circuits. The classical HH model yields a circuit (Chandler, FitzHugh and Cole, 1962) consisting of a parallel combination of capacitance, chord conductance (g_∞) and RL branches. The potassium RL branch forms a "parallel resonant" combination with the membrane capacitance. A parallel combination of resonant branches, containing *two* opposite susceptive elements all of a given type (i.e., parallel resonant or series resonant) will either show local minima, or local maxima, but not both. Thus, if membrane capacitance together with a single potassium RL branch is considered as a parallel resonant circuit which accounts for the observed impedance resonant peak in squid axon (with suppressed Na conduction), then the dip-producing phenomenon requires, in addition, either an RC or a series resonant branch. Consequently, all models that can possibly account for the low frequency mode (Fig. 1) must effectively introduce either an RC or a series resonant branch across the HH element.

Computations and Comparisons

Our criteria for fitting the data are the following:

1) The preservation of a substantial resonance at rest and depolarized potentials.

2) The correct voltage dependence of the zero crossings in the phase function.

3) Agreement with both the magnitude and phase functions at frequencies below 30 Hz.

We did not attempt to interpret these criteria quantitatively. One fit was considered better than another when there were unequivocal improvements in one or more of these criteria.

From extensive computer calculations involving systematic variation of each parameter in the model, a number of difficulties in attempts to fit the APS model (using modified α_n and β_n as well as the HH functions) were encountered, whether the model was corrected for $t_K I_K$ or not. These are summarized as follows. First, within a few orders of magnitude of reasonable parameter values, a dip between 10 and 20 Hz which appeared in the model (Fig. 5) did not recede satisfactorily as V_M was depolarized to between 10 and 20 mV, where there is no dip in the data. Second, the minimum of the dip would move from around 25 Hz at -9 mV to well over 100 Hz at $+9$ mV, whereas the resonant peak would

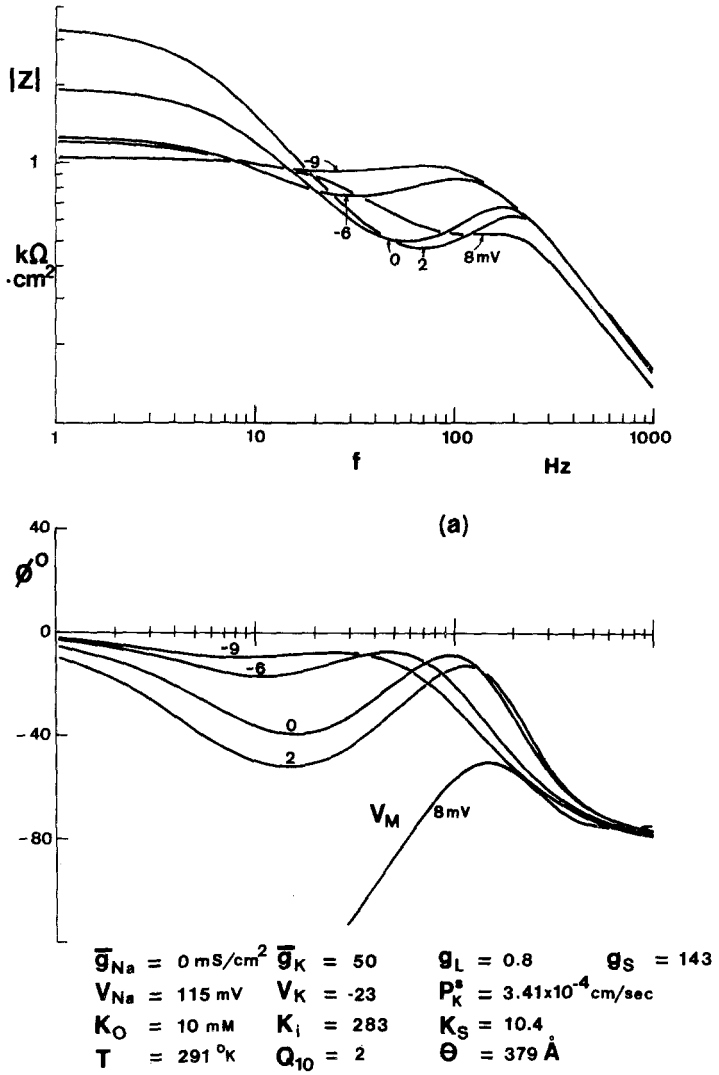

Fig. 5. Complex impedance with potential calculated from the APS (Adelman, Palti & Senft) model: (*a*) with modified values of HH parameters, (*b*) with modified values of HH parameters and an increase in θ (379 → 1000 Å) (the dip and resonance in $|Z|$ are more pronounced with potential variation), and (*c*) with significant changes in K_0, g_L, P_K^s and K_s from the values used in *b* to give a better approximation to the representative data in Fig. 1. Original HH values give much worse fits of impedance data in all cases. *c* represents the best approximation to the data obtained by systematic variation (10-fold) of all parameters in the APS model. Potentials in this and subsequent figures are relative to rest (0 mV = −60 mV absolute)

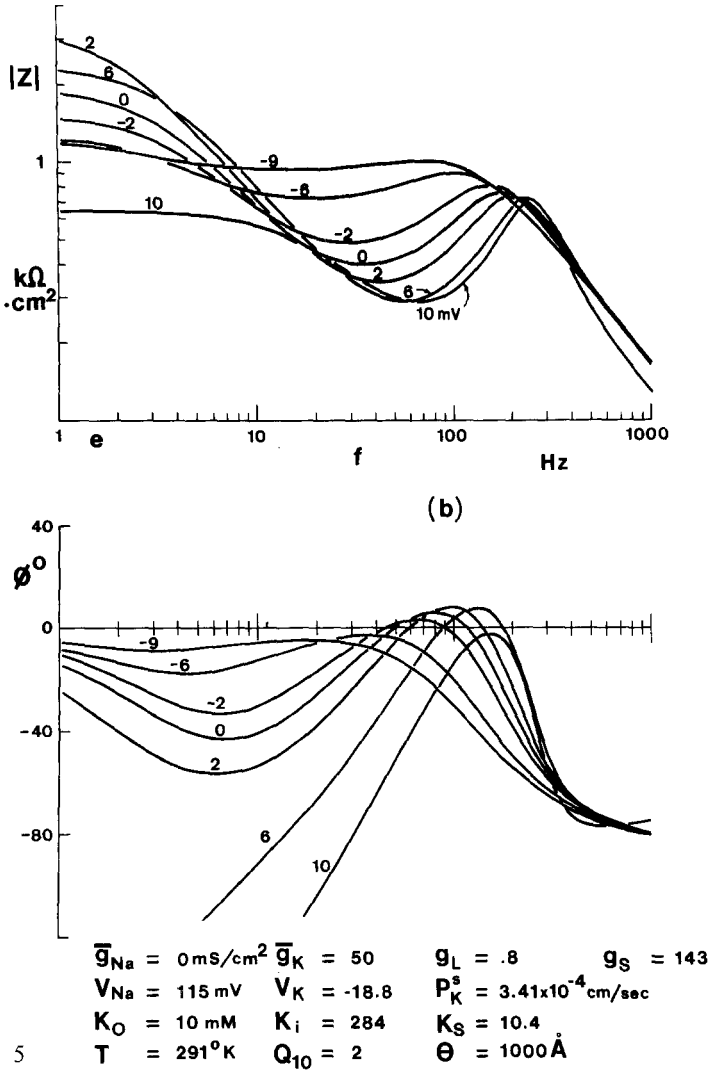

move from around 100 to 200 Hz. The first point is reminiscent of an earlier simulation (Fishman *et al.*, 1977*b*) with an RC element in series with the HH membrane, although the magnitude of the dip in the APS model went away rather better with depolarization. The second observation of a tendency for the dip to overtake the peak with depolarization appears also to have severe effects on the phase function, whereas the dip of a previous simulation moves much less and has a better phase fit (Fishman *et al.*, 1977*b*). A third observation is that at $\theta = 1000$ Å there is an increased tendency for the dip to overtake the peak, disappearing by depressing the latter. In the data, dips tend to move to the left rather

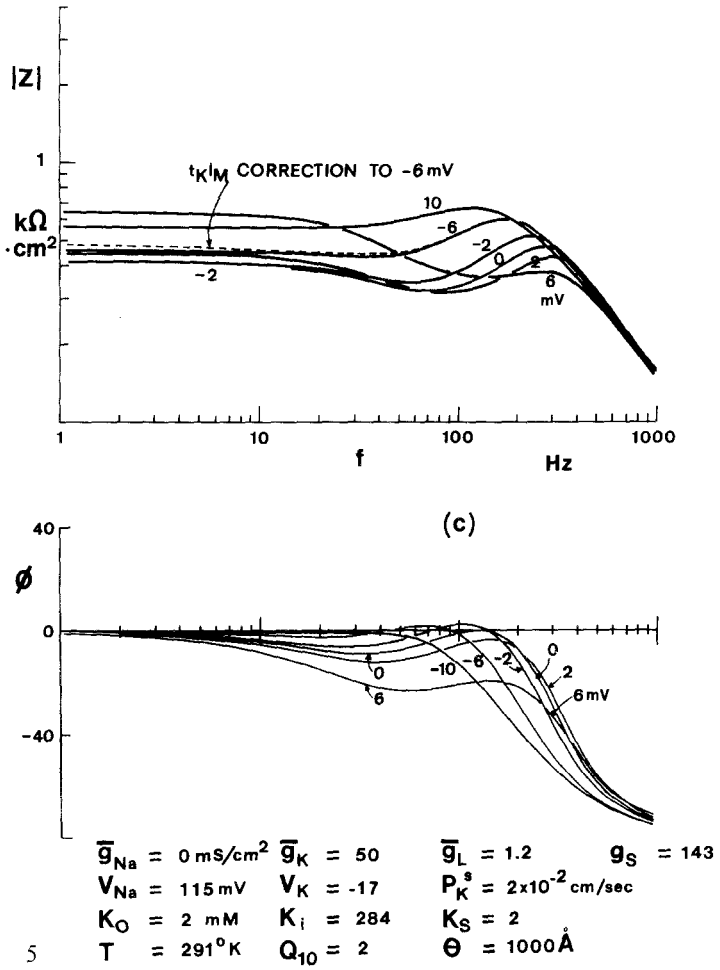

5

than the right, for membrane potentials increasing from -70 to -59 mV (Fig. 1). A related difficulty is the movement of the low frequency zero-crossing in phase: in data it moves to the left (Fig. 1), whereas in APS simulations it moves to the right with depolarization, when it exists at all, and the lowest zero-crossing (*see* -61 mV, Fig. 1) for APS has not been found in the present simulations, for a wide range of parameter values. In general, θ was found to be best at the APS nominal value of 379 Å, but g_L had to be increased to 0.8 mS/cm^2. A representative $t_K I_M$ correction is shown in Fig. 5*c* as a dashed line near the corresponding solid curve.

The potassium inactivation model could be adjusted to fit better, on the whole, than the APS model, with an inactivation parameter having

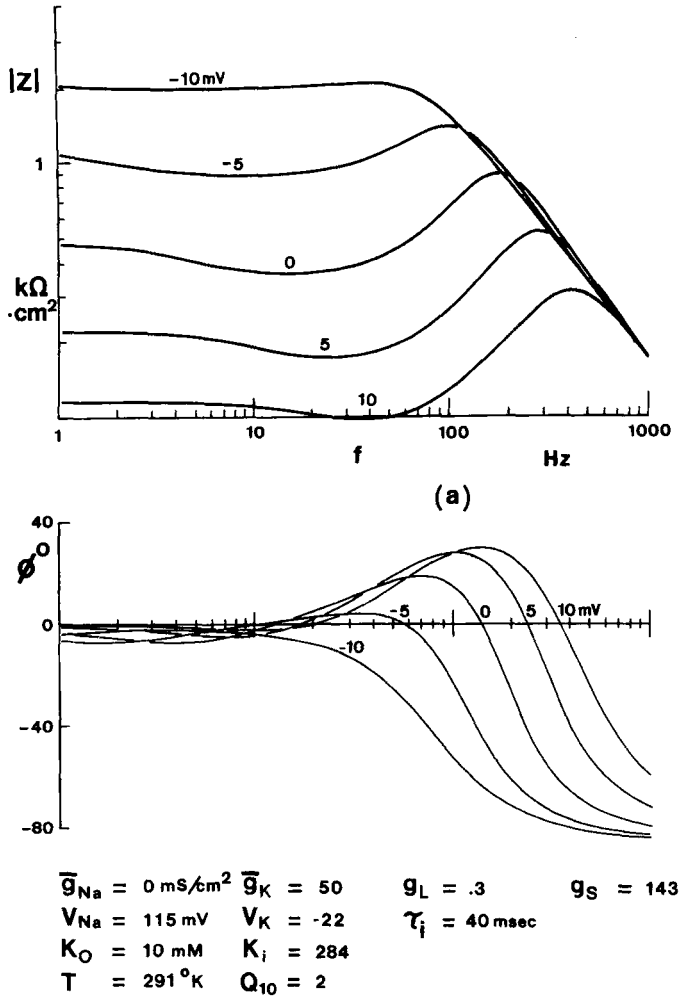

Fig. 6. Complex impedance with potential calculated from the potassium inactivation model (*a*) τ_i independent of potential, and (*b*) τ_i dependent on potential as in Fig. 4. In *a* middle zero crossing with potential is still incorrect; however, in *b* it moves to the left with small depolarization from −2 mV and the dip in |Z| disappears for extreme hyper- and depolarization as in the actual data (Fig. 1)

voltage-dependence as in Fig. 4 and with a *voltage-dependent time-constant*, also plotted in Fig. 4. With only the inactivation parameter voltage-dependent, the predicted dip moved to the right with depolarization (Fig. 6*a*) as with the models considered previously; but with the time-constant $\tau_i(V)$ decreasing with V, the magnitude could be fit closely (Fig. 6*b*). Unfortunately, the phase remained at best a qualitative fit, but correct at least as to the direction of movement of the middle zero-

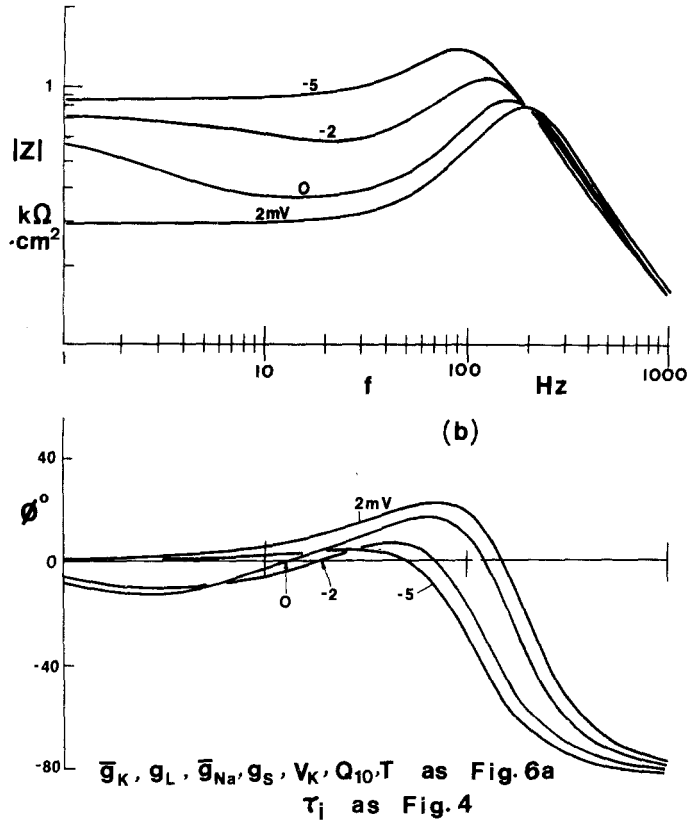

6

crossing. The explanation seems to be clear: inactivation produces an admittance branch which contributes essentially the feature of a first order process (a Lorentzian in terms of impedance squared-magnitude). This impedance "shoulder" tends to rise with hyperpolarization, eventually engulfing the constant component of the other potassium terms consisting of a resonance peak. If it rises vertically, it produces a dip over a finite interval, but one which moves to the right. If, on the other hand, the shoulder moves to the left as it subsides with depolarization, then the dip (and the zero-crossing) moves to the left. Without the voltage dependence of τ_i, the inactivation model suffers the same drawback as the Adam model and APS: the middle zero-crossing moves to the right.

The fits of the combined APS plus Adam potassium accumulation model [Eqs. (26)–(33)] were improved (in particular at frequencies below 10 Hz) over those obtained with APS alone by setting $\kappa = 80$ (Fig. 7). Over a small range ($-2 \rightarrow 5$ mV) the high frequency zero crossing in phase moves to the left with depolarization.

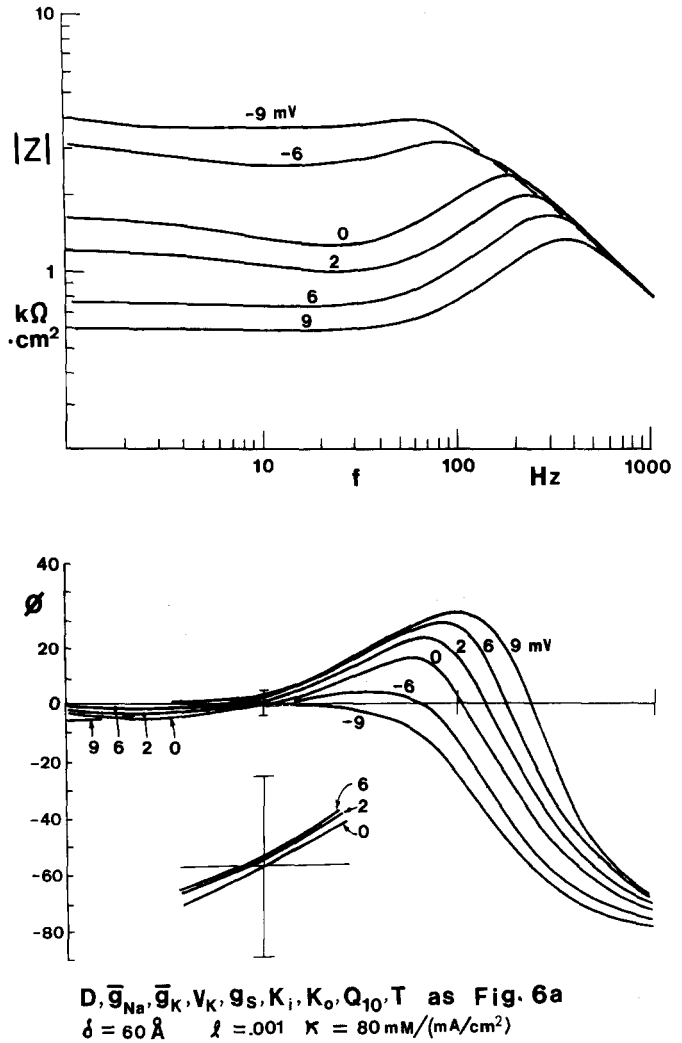

Fig. 7. Complex impedance with potential calculated from modified APS and Adam model with a diffusion barrier located at the outer limit of the SCL

Summary and Conclusions

The two classes of models considered are:

1) potassium accumulation in a phenomenological periaxonal space; (H1) (H2) (APS) (Adam)

2) potassium conductance inactivation.

These were tested in conjunction with a series resistance through the SCL. Over reasonable ranges of parameter values, the potassium accu-

mulation model tended to produce much larger dips and negative phase than the K conductance inactivation model and for depolarizations the dip did not disappear satisfactorily. Moreover, the dip due to potassium accumulation moved to the right with depolarization, whereas a voltage-dependent K inactivation rate constant could make the dip due to inactivation move to the left. Consequently, the phase form for inactivation was closer to data than for accumulation. However, when the accumulation was coupled to diffusion through the Schwann cell layer, significant improvements in the fit of admittance data were obtained. The best accumulation model suggests that, in addition to the accumulation and diffusion, there is a barrier to flow in the outer Schwann cell layer. However, at this point we do not have an explanation of this hypothetical barrier. We conclude that both 1 and 2 above can produce a low frequency mode in the complex impedance (admittance) of squid axon that is similar to that observed.

We thank Dr. Richard FitzHugh for his comments on the manuscript and an equivalent circuit representation of the K accumulation model and Dr. H. Richard Leuchtag for carefully reading the manuscript. In addition, we are grateful to Dr. K.S. Cole for discussions. This work was supported in part by NIH grants NS 11764 and NS 13778.

Appendix I

Derivation of the Potassium Admittance, $\hat{Y}_K$

At the SCL-PPS interface ($x=l$), $K=K_s$ and, from Eq. (34),

$$\delta K_s = \mu \delta K_{se} + C v \tag{A1}$$

where

$$\mu = (\cosh \gamma l)^{-1}$$

$$v = \gamma^{-1} \tanh \gamma l.$$

The Laplace transform of Eq. (25) gives

$$\delta K_{se} = \kappa F^{-1} \delta I_M.$$

Then, Eq. (A1) becomes

$$\delta K_s = \mu \kappa F^{-1} \delta I_M + C v$$

and

$$C = v^{-1} [\delta K_s - \mu \kappa F^{-1} \delta I_M]. \tag{A2}$$

Returning to Eq. (32),

$$[\partial \delta \mathrm{K}/\partial x]_{x=l} \equiv C = (FD)^{-1}[\delta I_{\mathrm{K}} - t_{\mathrm{K}} \delta I_M] - p\theta D^{-1} \delta \mathrm{K}_s$$

consequently,

$$v^{-1}[\delta \mathrm{K}_s - \mu \kappa F^{-1} \delta I_M] = (FD)^{-1}[\delta I_{\mathrm{K}} - t_{\mathrm{K}} \delta I_M] - p\theta D^{-1} \delta \mathrm{K}_s.$$

Solving for $\delta \mathrm{K}_s$, with $\delta I_M = \delta I_{\mathrm{K}}$ for simplicity,

$$\delta \mathrm{K}_s = F^{-1}[D v^{-1} + p\theta]^{-1} \delta I_{\mathrm{K}}(1+\mu') \tag{A3}$$

where $\mu' = \mu \kappa D v^{-1} - t_{\mathrm{K}}$.

From Eq. (26), the potassium conduction portion of the equation is obtained by setting $\bar{g}_{\mathrm{Na}} = g_L = 0$. Thus,

$$\delta I_{\mathrm{K}} = \left[\bar{g}_{\mathrm{K}} n_\infty^4 + \frac{4\bar{g}_{\mathrm{K}} n_\infty^3 A_n \tau_n (V_M - V_{\mathrm{K}})}{1 + p\tau_n}\right] \delta V_M - \bar{g}_{\mathrm{K}} n_\infty^4 RT(F\mathrm{K}_{ss})^{-1} \delta \mathrm{K}_s.$$

Substituting for $\delta \mathrm{K}_s$ from Eq. (A3) and collecting terms,

$$\delta I_{\mathrm{K}} \left[1 + \frac{\bar{g}_{\mathrm{K}} n_\infty^4 RT}{F^2 \mathrm{K}_{ss}} \frac{(1+\mu')}{(\mathrm{D} v^{-1} + p\theta)}\right] = \left[\bar{g}_{\mathrm{K}} n_\infty^4 + \frac{g_n}{1+p\tau_n}\right] \delta V_M.$$

Let $P_{\mathrm{K}} = D v^{-1} = D\gamma(\tanh \gamma l)^{-1}$

$$\begin{aligned} P_{\mathrm{K}}^M &\equiv \bar{g}_{\mathrm{K}} n_\infty^4 RT[F^2 \mathrm{K}_{ss}]^{-1}(1+\mu') \\ &= \bar{g}_{\mathrm{K}} n_\infty^4 RT[F^2 K_{ss}]^{-1}[1 + D\kappa\gamma(\sinh \gamma l)^{-1} - t_{\mathrm{K}}] \\ \tau_{\mathrm{K}} &\equiv \theta[P_{\mathrm{K}}^M + P_{\mathrm{K}}]^{-1}. \end{aligned}$$

Then

$$\delta I_{\mathrm{K}} \left[1 + \frac{P_{\mathrm{K}}^M}{(P_{\mathrm{K}} + p\theta)}\right] = \left[\bar{g}_{\mathrm{K}} n_\infty^4 + \frac{g_n}{1+p\tau_n}\right] \delta V_M.$$

The above yields the admittance

$$Y_{\mathrm{K}} = \frac{\delta I_{\mathrm{K}}}{\delta V_M} = \frac{P_{\mathrm{K}}}{P_{\mathrm{K}}^M + P_{\mathrm{K}}} \left[\bar{g}_{\mathrm{K}} n_\infty^4 + \frac{g_n}{1+p\tau_n}\right] \frac{(1 + p\theta/P_{\mathrm{K}})}{(1+p\tau_k)}. \tag{A4}$$

The effect of K accumulation vanishes as $l \to 0$, for which

$$P_{\mathrm{K}} \to \infty, \quad \frac{P_{\mathrm{K}}}{P_{\mathrm{K}}^M + P_{\mathrm{K}}} \to 1, \quad \tau_{\mathrm{K}} \to 0$$

and so

$$\hat{Y}_{\mathrm{K}} \to Y_{\mathrm{K}}^{\mathrm{HH}}.$$

In order to obtain $\hat{Y}_K$ in the form of Eq. (37*c*) we expand (A4) into partial fractions.

Let

$$a=\frac{P_K}{P_K^M+P_K}, \qquad \text{then } \theta/P_K=\tau_K/a.$$

Eq. (A4) becomes

$$\hat{Y}_K=a\left(\bar{g}_K n_\infty^4+\frac{g_n}{1+p\tau_n}\right)\frac{1+(p\tau_K/a)}{1+p\tau_k}$$

$$\hat{Y}_K(j\omega)=\frac{(\bar{g}_K n_\infty^4+g_n+j\omega\bar{g}_K n_\infty^4\tau_n)(a+j\omega\tau_K)}{(1+j\omega\tau_n)(1+j\omega\tau_K)} \tag{A5}$$

Let

$$\hat{Y}_K=\bar{g}_K n_\infty^4+\frac{A}{1+j\omega\tau_n}+\frac{B}{1+j\omega\tau_K} \tag{A6}$$

so that

$$\begin{aligned}(1+j\omega\tau_n)(1+j\omega\tau_K)\,\hat{Y}_K&=\bar{g}_K n_\infty^4(1+j\omega\tau_n)(1+j\omega\tau_K)\\&\quad+A(1+j\omega\tau_K)+B(1+j\omega\tau_n)\\&=(\bar{g}_K n_\infty^4+A+B)\\&\quad+j\omega[\tau_n(\bar{g}_K n_\infty^4+B)+\tau_K(\bar{g}_K n_\infty^4+A)]\\&\quad-\omega^2\bar{g}_K n_\infty^4\tau_n\tau_K.\end{aligned}$$

Therefore, from Eq. (A5), equating real and imaginary parts, we have

$$\bar{g}_K n_\infty^4+A+B=a(\bar{g}_K n_\infty^4+g_n)$$

and

$$\tau_n(\bar{g}_K n_\infty^4+B)+\tau_K(\bar{g}_K n_\infty^4+A)=(\bar{g}_K n_\infty^4+g_n)\tau_K+a\bar{g}_K n_\infty^4\tau_n.$$

Solving the above equations for A and B yields

$$A=g_n\left[1-(1-a)\frac{\tau_n}{\tau_n-\tau_K}\right]$$

$$B=(P_K^M/P_K)a[\bar{g}_K n_\infty^4(\tau_K-\tau_n)+g_n\tau_K](\tau_n-\tau_K)^{-1}.$$

If we let

$$\hat{g}_n=A, \qquad \hat{g}_K=B$$

then

$$\hat{Y}_K=\bar{g}_K n_\infty^4+\frac{\hat{g}_n}{1+j\omega\tau_n}+\frac{\hat{g}_K}{1+j\omega\tau_K}$$

which is Eq. (37c).

References

Adam, G. 1973. The effect of potassium diffusion through the Schwann cell layer on potassium conductance of the squid axon. *J. Membrane Biol.* **13**:353

Adelman, W.J., Jr., FitzHugh, R. 1975. Solutions of the Hodgkin-Huxley equations modified for potassium accumulation in a periaxonal space. *Fed. Proc.* **34**:1322

Adelman, W.J., Jr., Palti, Y. 1969*a*. The effects of external potassium and long duration voltage conditioning on the amplitude of sodium currents in the giant axon of the squid, *Loligo pealei*. *J. Gen. Physiol.* **53**:685

Adelman, W.J., Jr., Palti, Y. 1969*b*. The influence of external potassium on the inactivation of sodium currents in the giant axon of the squid, *Loligo pealei*. *J. Gen. Physiol.* **54**:589

Adelman, W.J., Jr., Palti, Y. 1972. Some relations between external cations and the inactivation of the initial transient conductance of the squid axon. *In:* Perspectives in Membrane Biophysics. D. P. Agin, editor. p. 101. Gordon & Breach, London

Adelman, W.J., Jr., Palti, Y., Senft, J.P. 1972. The role of periaxonal and perineuronal spaces in modifying ionic flow across neural membranes. *In:* Current Topics in Membranes and Transport. F. Bronner and A. Kleinzeller, editors. Vol. 3, p. 199. Academic Press, New York

Adelman, W.J., Jr., Palti, Y., Senft, J.P. 1973. Potassium ion accumulation in a periaxonal space and its effect on the measurement of membrane potassium ion conductance. *J. Membrane Biol.* **13**:387

Chandler, W.K., FitzHugh, R., Cole, K.S. 1962. Theoretical stability properties of a space-clamped axon. *Biophys. J.* **2**:105

Crank, J. 1975. The Mathematics of Diffusion. Clarendon, Oxford

Ehrenstein, G., Gilbert, D.L. 1966. Slow changes of potassium permeability in the squid giant axon. *Biophys. J.* **6**:553

Fishman, H.M., Moore, L.E., Poussart, D.J.M. 1975. Potassium-ion conduction noise in squid axon membrane. *J. Membrane Biol.* **24**:305

Fishman, H.M., Moore, L.E., Poussart, D. 1977*a*. Ion movements and kinetics in squid axon. II. Spontaneous electrical fluctuations. Ann. N.Y. Acad. Sci. **303**:399

Fishman, H.M., Poussart, D.J.M., Moore, L.E., Siebenga, E. 1977*b*. K^+ conduction description from the low frequency impedance and admittance of squid axon. *J. Membrane Biol.* **32**:255

FitzHugh, R. 1969. Mathematical models of excitation and propagation in nerve. *In:* Biological Engineering. H. Schwan, editor. p. 1. McGraw-Hill, New York

Frankenhaeuser, B., Hodgkin, A.L., 1956. The after-effects of impulses in the giant nerve fibres of *Loligo*. *J. Physiol.* (*London*) **131**:341

Geren, B.B., Schmitt, F.O. 1954. The structure of the Schwann cell and its relation to the axon in certain invertebrate nerve fibres. *Proc. Nat. Acad. Sci. USA* **40**:863

Goede, J. de, Vonk, M.W., Van den Berg, R.J., vanRijn, H., Verveen, A.A., 1977. *Ann. N. Y. Acad. Sci.* **303**:389

Hodgkin, A.L., Huxley, A.F., 1952. A quantitative description of membrane current and its application to conduction and excitation in nerve. *J. Physiol.* (*London*) **117**:500

Neumcke, B. 1971. Diffusion polarization at lipid bilayer membranes. *Biophysik* **7**:95

Poussart, D., Moore, L.E., Fishman, H.M. 1977. Ion movements and kinetics in squid axon. I. Complex admittance. *Ann. N. Y. Acad. Sci.* **303**:355

Villegas, R., Villegas, G.M. 1960. Characterization of the membranes in the giant nerve fibre of the squid. *J. Gen. Physiol.* **43**:73